Society of Petroleum Engineers

SPE-182707-MS

Low-dimensional tensor representations for the estimation of petrophysical reservoir parameters

E.Insuasty , Eindhoven University of Technology (EUT), P.M.J.Van den Hof, EUT, S.Weiland, EUT, J.D.Jansen, SPE, Delft University of Technology.

This paper was prepared for presentation at the SPE Reservoir Simulation Conference held in Montgomery, TX, USA 20–22 February 2017.

Abstract

In this work, the application of tensor methodologies for computer-assisted history matching of channelized reservoirs is explored. A tensor-based approach is used for the parameterization of petrophysical parameters to reduce the dimensionality of the parameter estimation problem. Building on the work of Afra and Gildin (2013); Afra et.al. (2014); Afra and Gildin (2016), permeability fields of multiple model realizations are collected in a tensor form which is subsequently decomposed to derive a low-dimensional representation of the dominant spatial structures in the models. This representation then is used to estimate an identifiable reduced set of parameters using an ensemble Kalman filter (EnKF) strategy. This approach is attractive for the parameter estimation of permeabilities because it increases the ability to represent channelized structures in the updates resulting in an improved predictive capacity of the history-matched models. In particular, channel continuity is better preserved than with a Principal Component Analysis (PCA) parameterization.

Introduction

Computer-assisted history matching (CAHM) has been successfully applied to reduce the level of uncertainty of the petrophysical properties by incorporating data-driven methods for parameter estimation. In this context, CAHM aims to assimilate production data by finding an updated set of model parameters (petrophysical parameters like permeabilities, porosities, net-to-gross ratios, etc.), such that the mismatch between production data and the model response is minimized. This has been a very prolific field of research and many algorithms have been developed in the last decades. For overviews we refer to the textbook by Oliver et al. (2008) and the review paper by Oliver and Chen (2011). Here we will use the Ensemble Kalman filtering method for which we refer to the textbook of Evensen (2009) and the review paper by Aanonsen et al. (2009).

Typically, the number of parameters to be estimated exceeds by far the number of available field measurements, and the parameter estimation problem becomes *ill-conditioned*, see e.g. Oliver et al. (2008). As the parameter estimation procedure is posed as an ill-conditioned optimization problem, there are usually several optimal solutions, i.e., there are multiple realizations of the petrophysical parameters that minimize the mismatch between the model output and the data. This implies the fact that while two history-matched reservoir realizations may look very different from the geological perspective, they may have very similar outputs in their response space. This phenomenon is illustrated in **Fig. 1**.

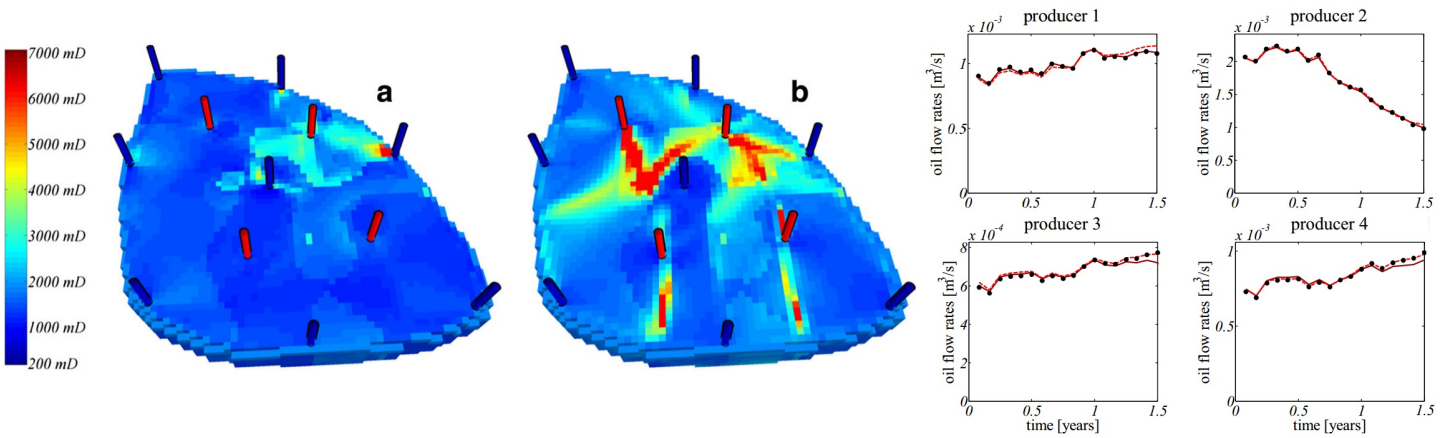

Figure 1: Rock permeability and well configuration of two updated reservoir models with very similar dynamical response (solid and dashed lines), adapted from van Essen et al. (2016).

From a Systems and Control perspective, a mathematical model that, when provided with different parameter sets, generates similar responses is usually classified as a non-identifiable model. Typically, reservoir models are non-identifiable, see e.g. Van Doren et al. (2009, 2011). In simple words, the petrophysical parameters are currently described at a level of detail which is too high to achieve a proper validation from the data. This problem is usually addressed through the use of a prior term with spatial correlations described with two-point statistics (a covariance matrix). However, spatial features that extend over many grid blocks, such as channels or faults, are not captured by such a description. In order to address this issue, several authors have developed parameterization methods of geological structures which include techniques based on sensitivity analysis and PCA: Oliver (1996); Reynolds et al. (1996); Tavakoli et al. (2010); Wavelets: Sahni et al. (2005); Channel parameterizations: Van Doren et al. (2011); Discrete Cosine Transform: Jafarpour et al. (2009, 2010); Pluri-Principal Component Analysis: Chen et al. (2016). Recently, there have been several developments aimed at preserving geological realism after the CAHM step, see, e.g., Vo and Durlofsky (2015). Sarma et al. (2008) have introduced the kernel PCA method, which can capture, to some extent, higher-order statistics, but involves the solution of a nontrival pre-imaging problem. From the perspective of CAHM, parameterizations are attractive because:

1. *Identifiability:* They increase the identifiability of the inverse modeling problem by estimating fewer parameters.

2. *Spatial structure:* They sometimes maintain spatial features such as channels or faults, that are not captured by two-point statistics (covariances).

Despite of these efforts, finding natural and simple representations of geological structures is still an active field of research. Tensor methodologies for parameter estimation constitute a relatively new subject in the reservoir simulation community, and Afra and Gildin (2013, 2014, 2016) and Afra et.al. (2014) have explored the application of tensor decompositions to represent permeability fields for parameter estimation. In this paper, we build on their work to achieve better predictive capabilities of updated channelized reservoir models in CAHM, while providing an explicit formulation of the tensor methodology for the parameterization of petrophysical parameters. We pursue this through the adaptation of an algorithm for parameter estimation that uses the low-dimensional tensor formulation of channelized permeability fields. In the next sections, we introduce the fundamental tensor tools, the type of parameterizations, the adapted ensemble algorithm for parameter estimation and a discussion of the results of the application of these developments in a test case.

Tensor modeling and decompositions

The low-rank approximation of matrices is well understood, see e.g. Eckart and Young (1936); Golub and Van Loan (2012), and recently there has been a huge development in the extension of low-rank approximations to multilinear arrays, see e.g. Chen and Saad (2009); De Lathauwer et al. (2000a,b); De Silva and Lim (2008); Kolda and Bader (2009); Lim (2004). This section introduces the concepts of multilinear algebra, algorithms and the tensor parameterization of petrophysical parameters.

Tensor representation of the petrophysical properties Let us consider a reservoir with a 2D rectangular geometry with $I \times J$ grid cells. Traditionally, the representation of the petrophysical parameters (permeability, porosity, etc.) has been in the form of an $(I \cdot J \times 1)$ vector. Alternatively, if the spatial grid has a Cartesian structure, and if there is an ensemble of models, one can collect R realizations θ of size $I \times J$, and represent this data object in a three-dimensional array $\mathcal{S}$ of size $I \times J \times R$. That is, the ensemble of realizations is represented as a multidimensional array $\mathcal{S} \in \mathbb{R}^{I \times J \times R}$. Such a multidimensional array is called a *tensor* and can be viewed as the natural generalization of vectors and matrices to higher dimensional objects. For an ensemble of 2D channelized permeability fields, a three-dimensional array is schematically depicted in **Fig. 2**.

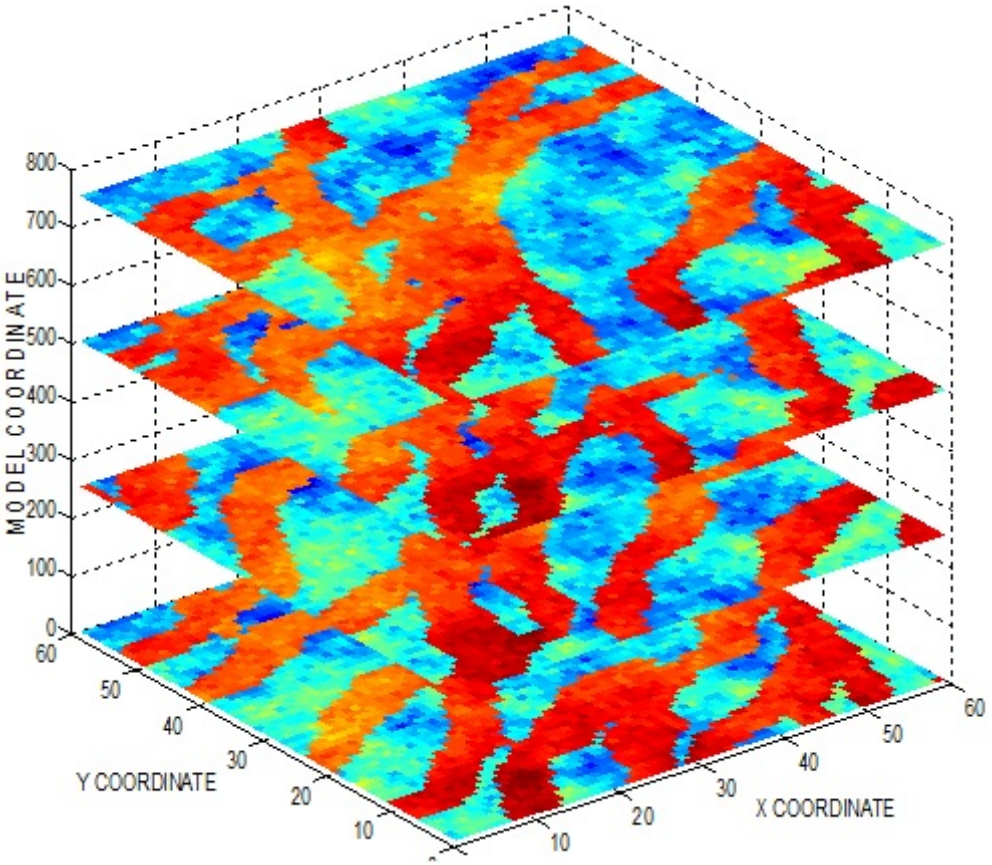

Figure 2: Schematic of the tensor representation of a petrophysical property (permeability) of an ensemble of channelized models. The horizontal axes represent spatial coordinates and the vertical axis the model coordinate.

In the tensor representation, the geometrical and spatial structures remain intact. In addition, the multilinear domain allows extensions of classical matrix decompositions to tensors, and the notions of approximations and low-rank approximations can be also defined in the tensor framework.

Fundamentals of linear and multilinear algebra Tensors are the multilinear extension of vectors and matrices and can be represented as multilinear arrays and, similar to the matrix case, tensors can be interpreted as multi-

linear mappings. With this interpretation, a tensor induces a multilinear mapping $\mathcal{S} : \mathbb{R}^{I_1} \times \mathbb{R}^{I_2} \times \cdots \times \mathbb{R}^{I_N} \to \mathbb{R}$. Let $\mathcal{T}_N$ be the set of all N-way mappings $\mathbb{R}^{I_1} \times \mathbb{R}^{I_2} \times \cdots \times \mathbb{R}^{I_N} \to \mathbb{R}$, then $\mathcal{T}_N$ becomes a vector space when it is equipped with additive and multiplicative properties, see e.g. van Belzen (2011); Van Belzen and Weiland (2012). Given two tensors $\mathcal{S}, \mathcal{R} \in \mathcal{T}_N$, the following properties can be defined:

- Additivity: $\mathcal{Q} = \mathcal{S} + \mathcal{R} \in \mathcal{T}_N$, where the $(i_1 i_2 \cdots i_N)$th element of $\mathcal{Q}$, i.e. $q_{i_1 i_2 \cdots i_N} = s_{i_1 i_2 \cdots i_N} + r_{i_1 i_2 \cdots i_N}$, the sum of the $(i_1 i_2 \cdots i_N)$th elements of $\mathcal{S}$ and $\mathcal{R}$.
- Tensor multiplication by a scalar: $\mathcal{P} = \alpha\mathcal{S} \in \mathcal{T}_N$ for any $\alpha \in \mathbb{R}$, where the $(i_1 i_2 \cdots i_N)$th element of $\mathcal{P}$, i.e. $p_{i_1 i_2 \cdots i_N} = \alpha s_{i_1 i_2 \cdots i_N}$.

It is important to understand that the elements of $\mathcal{S}$, i.e. $s_{i_1 i_2 \cdots i_N}$ are defined with respect to a set of basis functions:

$$\{f_1^{i_1}, \text{ for } i_1 = 1, \cdots, I_1\}, \cdots \{f_N^{i_N}, \text{ for } i_N = 1, \cdots, I_N\}. \tag{1}$$

If the vector space $\mathcal{T}_N$ is equipped with an inner product, it allows the definition of a normed space. With $\mathcal{S}, \mathcal{R} \in \mathcal{T}_N$, the inner product $\langle \cdot, \cdot \rangle$ between $\mathcal{S}$ and $\mathcal{R}$ is defined as:

$$\langle \mathcal{S}, \mathcal{R} \rangle := \sum_{i_1=1}^{I_1} \cdots \sum_{i_N=1}^{I_N} \sum_{j_1=1}^{I_1} \cdots \sum_{j_N=1}^{I_N} s_{i_1 i_2 \cdots i_N} r_{j_1 j_2 \cdots j_N} \langle f_1^{i_1}, f_1^{j_1} \rangle \cdots \langle f_N^{i_N}, f_N^{j_N} \rangle \tag{2}$$

Hence, an induced tensor norm can be defined as $\|\mathcal{S}\|_F = \sqrt{\langle \mathcal{S}, \mathcal{S} \rangle}$, known as the Frobenious norm, which is equal to

$$\|\mathcal{S}\|_F = \sqrt{\sum_{i_1=1}^{I_1} \cdots \sum_{i_N=1}^{I_N} \sum_{j_1=1}^{I_1} \cdots \sum_{j_N=1}^{I_N} s_{i_1 i_2 \cdots i_N}}, \tag{3}$$

for the special case when the basis functions in Eq. 1 are orthogonal.

Tensor decompositions and approximations The most general formulation of a tensor decomposition is provided by the Tucker decomposition, see, e.g., the work of Tucker (1966) and Kolda and Bader (2009), where the tensor $\mathcal{S}$ is represented by the multiplication of the elements of a full core tensor with rank 1 tensors, defined by the basis functions for each of the tensor coordinate spaces. The Tucker decomposition can be defined as:

$$\mathcal{S} = \sum_{i=1}^{I} \sum_{j=1}^{J} \sum_{r=1}^{R} \sigma_{ijr} \varphi_i \otimes \psi_j \otimes \vartheta_r = \sum_{i=1}^{I} \sum_{j=1}^{J} \sum_{r=1}^{R} \sigma_{ijr} \Theta_{ijr}, \tag{4}$$

where the scalars $\sigma_{ijr} \in \mathbb{R}$ are the elements of the so called *core tensor* of size $I \times J \times R$ and where

$$\Theta_{ijr} := \varphi_i \otimes \psi_j \otimes \vartheta_r \tag{5}$$

is the outer product of vectors $\varphi_i \in \mathbb{R}^I$, $\psi_j \in \mathbb{R}^J$ and $\vartheta_r \in \mathbb{R}^R$. This makes Θ_{ijr} a rank-one 3-way tensor. In such a representation, the sets $\{\varphi_i\}_{i=1}^I$, $\{\psi_j\}_{j=1}^J$ and $\{\vartheta_r\}_{r=1}^R$ are usually taken as a *basis* of $\mathbb{R}^I$, $\mathbb{R}^J$ and $\mathbb{R}^R$, respectively, and the Tucker decomposition, Eq. 4 is viewed as a representation of the tensor with respect to these bases. More precisely, the rank-one 3-way tensor Θ_{ijr} is a multilinear mapping $\Theta_{ijr} : \mathbb{R}^I \times \mathbb{R}^J \times \mathbb{R}^R \to \mathbb{R}$ defined as

$$\Theta_{ijr}(\varphi, \psi, \vartheta) := \langle \varphi_i, \varphi \rangle \langle \psi_j, \psi \rangle \langle \vartheta_r, \vartheta \rangle \tag{6}$$

which is a product of inner products in $\mathbb{R}^I$, $\mathbb{R}^J$ and $\mathbb{R}^R$. At this stage, it is important to observe that the mapping Θ_{ijr}, defined in this way, is linear in each of its argument. Moreover, if the bases $\{\varphi_i\}_{i=1}^I$, $\{\psi_j\}_{j=1}^J$ and $\{\vartheta_r\}_{r=1}^R$ are all orthonormal sets (that is, $\langle \varphi_{i'}, \varphi_{i''} \rangle = 1$ if $i' = i''$ and zero otherwise for vectors $\{\varphi_i\}_{i=1}^I$), it follows that

$$\mathcal{S}(\varphi_{i_0},\psi_{j_0},\vartheta_{r_0}) = \sum_{i=1}^{I}\sum_{j=1}^{J}\sum_{r=1}^{R}\sigma_{ijr}\Theta_{ijr}(\varphi_{i_0},\psi_{j_0},\vartheta_{r_0}) = \sigma_{i_0 j_0 r_0} \tag{7}$$

for any triple of indices (i_0, j_0, r_0) with $1 \le i_0 \le I$, $1 \le j_0 \le J$ and $1 \le r_0 \le R$. In words, this says that the entries of the core tensor represent the tensor $\mathcal{S}$ when evaluated at its (orthonormal) basis vectors. If the bases are orthonormal, then this observation naturally identifies the entries $\sigma_{i_0 j_0 r_0}$ of the core tensor with the evaluation of the tensor $\mathcal{S}$ at its (i_0, j_0, r_0)th basis element. When evaluating $\mathcal{S}$ at vectors which are not basis functions, then the multilinear functional $\mathcal{S} : \mathbb{R}^I \times \mathbb{R}^J \times \mathbb{R}^R \to \mathbb{R}$ defined in Eq. 7 and operating over the vectors $(\varphi, \psi, \vartheta)$ changes its representation, and produces:

$$\mathcal{S}(\varphi,\psi,\vartheta) = \sum_{i=1}^{I}\sum_{j=1}^{J}\sum_{r=1}^{R}\sigma_{ijr}\langle\varphi_i,\varphi\rangle\,\langle\psi_j,\psi\rangle\,\langle\vartheta_r,\vartheta\rangle. \tag{8}$$

A particular case of the Tucker decomposition is the canonical polyadic (CP) decomposition, also known as the PARAFAC decomposition, and has been successfully applied in the field of chemometrics, see e.g. Bro (1997); Harshman (1970); Harshman and Lundy (1994). In the CP decomposition the core tensor is "diagonal", i.e., the elements of the core tensor $\sigma_{ijr} \neq 0$ for $i = j = r$, and $\sigma_{ijr} = 0$ otherwise.
For the Tucker decomposition, a low-rank approximation of $\mathcal{S}$ can be obtained by decomposing Eq. 4 according to $\mathcal{S} = \widehat{\mathcal{S}} + \overline{\mathcal{S}}$ where, for $\widehat{I} \le I$, $\widehat{J} \le J$, $\widehat{R} \le R$, the tensor

$$\widehat{\mathcal{S}} := \sum_{i=1}^{\widehat{I}}\sum_{j=1}^{\widehat{J}}\sum_{r=1}^{\widehat{R}}\sigma_{ijr}\Theta_{ijr} \tag{9}$$

is viewed as the approximation of $\mathcal{S}$ to its *modal-rank* $(\widehat{I},\widehat{J},\widehat{R})$ truncation and where $\overline{\mathcal{S}} := \mathcal{S} - \widehat{\mathcal{S}}$ is viewed as the corresponding approximation error. The size of the approximation error is measured in Frobenius norm and satisfies

$$\| \mathcal{S} - \widehat{\mathcal{S}} \|_F^2 \quad = \quad \| \mathcal{S} \|_F^2 - \sum_{i=1}^{\widehat{I}}\sum_{j=1}^{\widehat{J}}\sum_{r=1}^{\widehat{R}}\sigma_{ijr}^2 = \sum_{i=\widehat{I}+1}^{I}\sum_{j=\widehat{J}+1}^{J}\sum_{r=\widehat{R}+1}^{R}\sigma_{ijr}^2, \tag{10}$$

provided that the bases $\{\varphi_i\}_{i=1}^I$, $\{\psi_j\}_{j=1}^J$ and $\{\vartheta_r\}_{r=1}^R$ are orthonormal sets. The Frobenius norm of tensors in Eq. 10 is used to compute a relative approximation error related to the tensor approximation as follows:

$$e_{rel} = \frac{||\mathcal{S} - \widehat{\mathcal{S}}||_F}{||\mathcal{S}||_F} = \sqrt{\frac{\sum_{i=\hat{I}+1}^{I}\sum_{j=\hat{J}+1}^{J}\sum_{r=\hat{R}+1}^{R}\sigma_{ijr}^2}{\sum_{i=1}^{I}\sum_{j=1}^{J}\sum_{r=1}^{R}\sigma_{ijr}^2}}. \tag{11}$$

Algorithms for tensor decompositions Clearly, the approximation accuracy of Eq. 9 depends on the choice of basis vectors φ_i, ψ_j, and ϑ_r, their ordering and the elements in the core tensor. There exist many algorithms to select these bases in such a way that the approximation error, Eq. 10 is small or minimized.
The problem of finding these sets can be formulated as the optimization problem

$$\min_{\{\varphi_i\}_{i\le\widehat{I}},\{\psi_j\}_{j\le\widehat{J}},\{\vartheta_r\}_{r\le\widehat{R}}} \left\| \mathcal{S} - \sum_{i=1}^{\widehat{I}}\sum_{j=1}^{\widehat{J}}\sum_{r=1}^{\widehat{R}}\sigma_{ijr}\varphi_i\otimes\psi_j\otimes\vartheta_r \right\|_F \tag{12}$$

which is to be solved subject to the constraint that the basis elements $\{\varphi_i \mid 1 \le i \le \widehat{I}\}$, $\{\psi_j \mid 1 \le j \le \widehat{J}\}$ and $\{\vartheta_r \mid 1 \le r \le \widehat{R}\}$ are orthonormal.

This problem has an analytic solution only for the case where $(\hat{I},\hat{J},\hat{R}) = (1,1,1)$. For all other cases one has to resort to numerical approximations. Several algorithms have been proposed to compute tensor decompositions using orthonormal basis functions. The *High Order SVD* (HOSVD) proposed by De Lathauwer et al. (2000a) was the first extension of the classical SVD to the tensor domain and the methodology is based on an unfolding procedure of tensors. The *High Order Orthogonal Iteration* (HOOI) by De Lathauwer et al. (2000b), the *Tensor SVD* proposed by Weiland and Van Belzen (2010), *Maximum Singular Value Modal Rank* (MSVM) and the *Single Directional Modal-rank decomposition* (SDM) by Shekhawat and Weiland (2014) compute singular values (elements of the core tensor) and basis vectors in a sequential way, where the singular values and vectors depend on a search direction at every decomposition level $(\widehat{I},\widehat{J},\widehat{R})$. The tensor SVD, MSVM and SDM algorithms keep the tensor structure intact in such a decomposition procedure. In this paper, we consider the *Tucker modal-rank* type of decomposition, see Kolda and Bader (2009), which achieves orthonormal sets $\{\varphi_i\}_{i=1}^{I}$, $\{\psi_j\}_{j=1}^{J}$ and $\{\vartheta_r\}_{r=1}^{R}$. There are several tensor toolboxes available for the Matlab platform, like the Matlab Tensor toolbox, see, e.g., Bader et al. (2015) and the Tensorlab, see, e.g., Vervliet et al. (2016). In this work we have implemented the HOSVD using tensor functions from the Matlab Tensor Toolbox, see, e.g., Bader et al. (2015).

Tensor approximations of permeability fields In order to illustrate the use of tensor decompositions to approximate the petrophysical parameters of an ensemble of realizations, we analyze the performance of the classical SVD and tensor approaches for low-dimensional representations of permeability fields. Let us consider an ensemble of 3D geological models with a geological structure consisting of a network of fossilized meandering channels of high permeability. The data set has been uploaded to the 4TU.Datacentrum repository and can be accessed by external users, see Jansen et al. (2014). A view of the first layer of one of the geological realizations from the ensemble is depicted in **Fig. 3**. Note that here we use the full square realization with all grid blocks, whereas in the original model several grid blocks were declared void in order to modify the reservoir shape. The realizations are composed of 25200 grid blocks that are $8 \times 8 \times 4$m in size, and have dimensions of $480 \times 480 \times 28$m and 7 geological layers, and we consider $R = 100$ realizations.

We construct a 4D tensor $\mathcal{S}$ of size $60 \times 60 \times 7 \times 100$, where the x, y, z and model dimensions correspond to the first, second, third and fourth tensor coordinates accordingly. Hence, the tensor $\mathcal{S}$ can be decomposed as in Eq. 4:

$$\mathcal{S} = \sum_{i=1}^{60}\sum_{j=1}^{60}\sum_{z=1}^{7}\sum_{r=1}^{100} \sigma_{ijkr}\varphi_i \otimes \psi_j \otimes \chi_z \otimes \vartheta_r. \tag{13}$$

For instance, the permeability fields in tensor $\mathcal{S}$ are described by $I = 60$ basis functions, which are vectors $\varphi \in \mathbb{R}^{60}$, for the x coordinate; $J = 60$ basis functions, which are vectors $\psi \in \mathbb{R}^{60}$, for the y coordinate; $Z = 7$ basis functions, which are vectors $\chi \in \mathbb{R}^{7}$, for the z coordinate; and $R = 100$ basis functions, which are vectors $\vartheta \in \mathbb{R}^{100}$, for the model coordinate. We compute low-rank approximations $\widehat{\mathcal{S}}$ of the original permeability pattern by truncating the sums in Eq. 13 as follows: $\{\varphi_i\}_{i=1}^{\widehat{I}=20}$ for the x coordinate, $\{\psi_j\}_{j=1}^{\widehat{J}=20}$ for the y coordinate, $\{\chi_z\}_{z=1}^{\widehat{Z}=1}$ for the z coordinate and $\{\vartheta_r\}_{r=1}^{\widehat{R}=100}$ for the model coordinate, leading to a modal rank approximation of $(15,35,1,100)$. The quality of the tensor approximation is compared with the classical low-rank approximation provided by the SVD, where the vector representations of the petrophysical properties are collected in a matrix $\mathbf{S}$ of size $I \cdot J \cdot Z \times R$, and a low-rank approximation of $\mathbf{S}$ is constructed by selecting a few basis functions. The visualization of one realization and the SVD and tensor approximation are depicted in Fig. 3. The results in Fig. 3 indicate that the rank of the SVD approximations has to be increased to 60 in order to reconstruct adequately the general patterns of the permeability fields. One relevant aspect comes from the amount of information required to approximate the rock patterns, measured in megabytes. The tensor $\mathcal{S}$ and the matrix $\mathbf{S}$ have a memory size of 20.16MB, and the basis functions and the core tensor in Eq. 13 for the tensor approximation of modal rank $(15,35,1,100)$ have a memory size of 0.53MB in total, which corresponds to the 2.6% of the size of the original tensor $\mathcal{S}$. If we

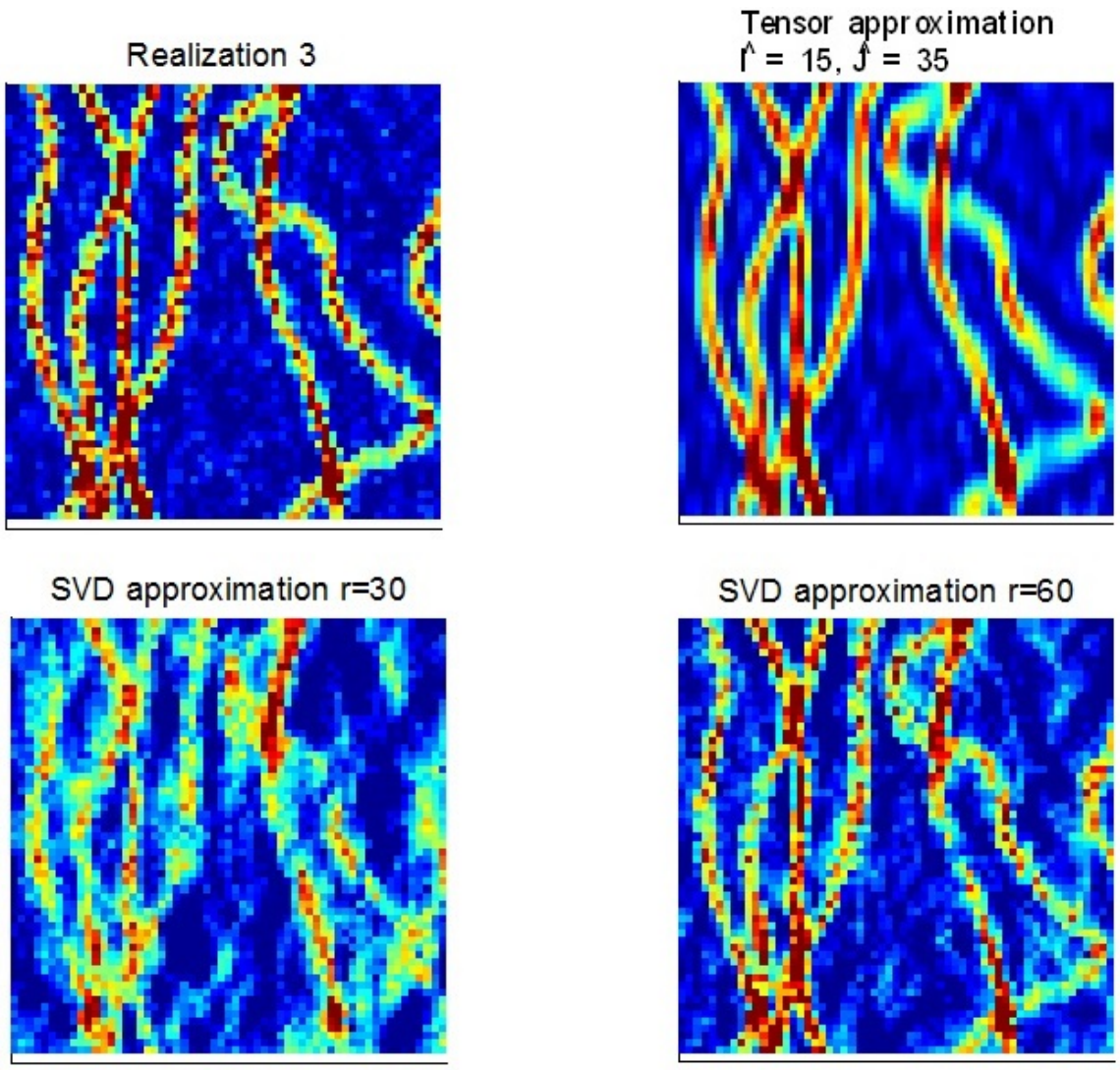

Figure 3: Low rank approximations using classical SVD and tensor decompositions.

check the memory size of the basis functions and singular value matrices required to compute the low-rank SVD approximation of rank 60 of **S**, we find that this is 12.17MB, which corresponds to the 60.3% of the memory size of the original matrix **S**. This result demonstrates the compression capabilities of tensor decompositions. This characteristic will be used in the next sections to find low-order parameterizations of permeability fields.

The surface plot of the **Fig. 4** depicts the relative error as defined in Eq. 10 as a function of the number of spatial basis functions in the x and y coordinates. From the surface plot it is possible to visualize that increasing the number of basis functions for the y coordinate has a bigger impact on the quality of the approximation than increasing the number of basis functions in the x coordinate. This result has a physical interpretation since the channel orientation is along the y coordinate. To confirm the directional relevance of the basis functions in the coordinate that is aligned with the channels, we have depicted in Fig. 4 the relative error when fixing the number of basis functions to 60 for the x or y coordinates and varying the number of basis functions for the other coordinate. The plot confirms the observation and suggest that the basis functions in the y coordinate are more relevant to approximate the features of the channels aligned with the y coordinate. For instance, tensor decompositions can be used for directional approximations that emphasize geological features like channels which are aligned with a particular spatial coordinate, and provide a framework to approximate petrophysical parameters in a more efficient way than classical SVD methods.

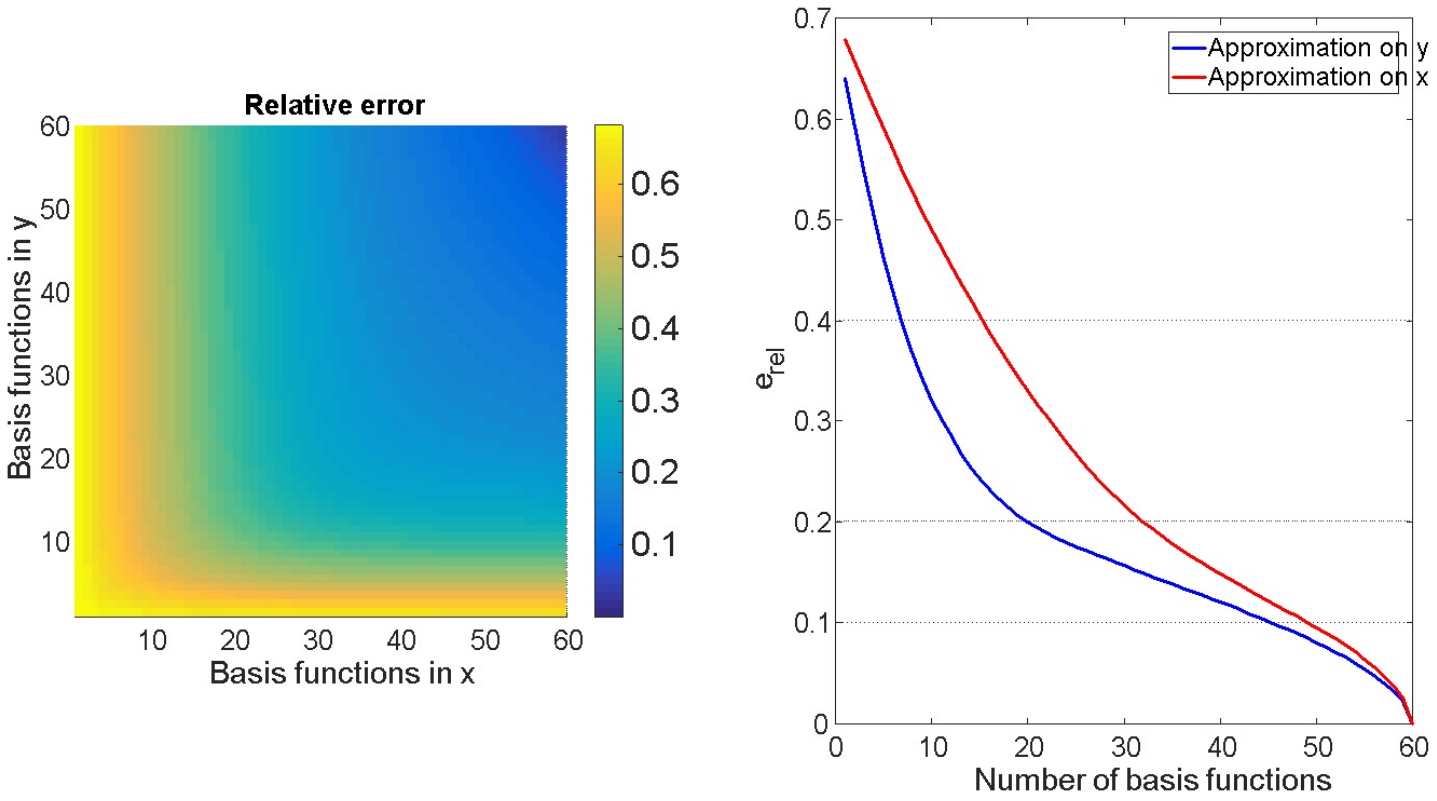

Figure 4: Relative error of the approximations. Left: Relative error as a function of the basis functions in the x and y coordinates. The color-scale corresponds to magnitude. Right: Relative error fixing the number of basis functions in one coordinate, and varying the number of basis functions in the other.

Methods like the DCT parameterizations, see e.g. Jafarpour et al. (2009), use real cosine functions to define infinite series expansions of the permeability fields, while assuming that the most relevant geological features are preserved in the low frequency modes. Despite that this method is computationally efficient due to the fast algorithms for Fourier transforms, the approximation error is minimal if and only if the number of basis functions (cosines) tends to infinity, and in theory, it usually requires a large number of Fourier modes to capture relevant geological features. In practice, DCT-based approximations have a good performance while using a few set of basis functions, but no error estimates can be derived from the approximations. The tensor approach to the approximation of permeability fields computes the optimal basis functions which guarantee the best approximation with the computed basis functions, and error estimates can be easily computed using Eq. 11. In addition, it provides a framework for approximating geological features which are aligned with one specific spatial coordinate.

Tensor parameterizations of permeability fields

Previously, we have exemplified the benefits of implementing tensor representations and decompositions of petrophysical parameters to extract the most relevant geological features in low-dimensional spaces. In this section, we propose a low-dimensional parameterization of the petrophysical parameters based on the tensor decomposition described in Eq. 4, which can be incorporated in parameter estimation routines. To illustrate, suppose now that the Tucker tensor decomposition is applied to the data corresponding to an ensemble of two-dimensional rectangular permeability fields. The permeability field of the mth realization θ_m is then represented as a *matrix* of dimension $I \times J$. A number of R realizations of petrophysical parameters θ_m is stored in an order-3 tensor $\mathcal{S}$ of size $I \times J \times R$. This tensor is approximated as in Eq. 9, and results in the approximate sample $\widehat{\theta}_m$ of the permeability field defined by the order-2 tensor

$$\widehat{\theta}_m = \widehat{\mathcal{S}}(\cdot,\cdot,\mathbf{e_m}) = \sum_{i=1}^{\widehat{I}}\sum_{j=1}^{\widehat{J}}\sum_{r=1}^{\widehat{R}} \sigma_{ijr}\langle\vartheta_r,\mathbf{e_m}\rangle\,\varphi_i\otimes\psi_j = \sum_{i=1}^{\widehat{I}}\sum_{j=1}^{\widehat{J}} \alpha_{ij}^m\varphi_i\otimes\psi_j \tag{14}$$

where $\mathbf{e_m}$ is the mth standard unit vector in $\mathbb{R}^R$ and where $\alpha_{ij}^m := \sum_{r=1}^{\widehat{R}}\sigma_{ijr}\langle\vartheta_r,\mathbf{e_m}\rangle$ are real-valued coefficients in the expansion in Eq. 14 of a (rank 1) two-dimensional permeability field. The coefficients α_{ij}^m are linear combinations of the mth elements of the basis functions in the set $\{\vartheta_r\}_{r=1}^{\widehat{R}}$, i.e., $\alpha_{ij}^m = \sum_{r=1}^{\widehat{r}}\sigma_{ijr}\,\vartheta_r^{(m)}$, where $\vartheta_r^{(m)} = \langle\vartheta_r,\mathbf{e_m}\rangle$. The expression in Eq. 14 is a tensor representation of the permeability fields, where all realizations of the ensemble share the same spatial basis functions defined by $\varphi_i\otimes\psi_j$. In this tensor form, the realizations are characterized by the set of coefficients α_{ij}. This representation induces a parameterization of the ensemble if we allow the coefficients α_{ij} to be free parameters. In the next section, we explore the use of this induced parameterization for parameter estimation.

EnKF for parameter estimation using tensor parameterizations

The objective of CAHM is to update the model parameters through assimilating the information contained in measurements taken during the operation of the oil reservoir, which typically are the production rates and bottom-hole or tubing head pressures at the well locations. Afra and Gildin (2014) have introduced an Alternating Least Squares type of decomposition, used for the inference of permeability fields. In this section, we incorporate the tensor parameterization described in the previous section into the EnKF scheme. Let us consider the reservoir model:

$$\mathbf{x_{k+1}} = \mathbf{f}(\mathbf{x_k},\mathbf{u_k},\theta), \tag{15}$$

where $\mathbf{f}$ is a vector-valued nonlinear function of the states $\mathbf{x_k}$, the petrophysical parameters θ and the inputs $\mathbf{u_k}$. Let $\mathbf{d_k^{sim}} = \mathbf{h}(\mathbf{x_k},\mathbf{u_k})$ be the nonlinear output operator. Using the representation in Eq. 14, the petrophysical parameters can be approximated by $\widehat{\theta} = \sum_{i=1}^{\widehat{I}}\sum_{j=1}^{\widehat{J}}\alpha_{ij}\varphi_i\otimes\psi_j$, and can be characterized by the set of parameters α_{ij}. Let all the parameters α_{ij} be collected in the vector $\mathbf{a}\in\mathbb{R}^{\widehat{I}.\widehat{J}}$, and let us consider the augmented state vector $\mathbf{z_k}$:

$$\mathbf{z_{k+1}} = \begin{bmatrix}\mathbf{x_{k+1}}\\ \mathbf{a}\\ \mathbf{d_{k+1}^{sim}}\end{bmatrix} = \bar{\mathbf{f}}(\mathbf{z_k},\mathbf{u_k}) = \begin{bmatrix}\mathbf{f}(\mathbf{x_k},\mathbf{u_k},\widehat{\theta})\\ \mathbf{a}\\ \mathbf{h}(\mathbf{x_k},\mathbf{u_k})\end{bmatrix}, \tag{16}$$

with augmented output vector $\mathbf{y_k}$:

$$\mathbf{y_{k+1}} = \mathbf{H z_k} = \begin{bmatrix}\mathbf{0} & \mathbf{0} & \mathbf{I}\end{bmatrix}\begin{bmatrix}\mathbf{f}(\mathbf{x_k},\mathbf{u_k},\widehat{\theta})\\ \mathbf{a}\\ \mathbf{h}(\mathbf{x_k},\mathbf{u_k})\end{bmatrix}. \tag{17}$$

The EnKF approach follows the sequential steps of the classical KF, but uses an ensemble of R parameterizations of the realizations $\Omega = \{\mathbf{a^1},\mathbf{a^2},\cdots,\mathbf{a^R}\}$ to update the mean and covariance of the augmented state $\mathbf{z}$:

1. *Forecast*: For every model realization in the set Ω, the forecast of the ensemble of augmented states is generated, and the matrix $\Xi_{\mathbf{k+1}}^{\mathbf{f}} = \left[\mathbf{z_{k+1}^{1,f}},\mathbf{z_{k+1}^{2,f}},\cdots,\mathbf{z_{k+1}^{R,f}}\right]$ is constructed according to:

$$\mathbf{z}^{\mathbf{i,f}}_{\mathbf{k+1}} = \begin{bmatrix} \mathbf{x}^{\mathbf{i,f}}_{\mathbf{k+1}} \\ \mathbf{a}^{\mathbf{i,f}}_{\mathbf{k+1}} \\ \mathbf{d}^{\mathbf{sim,i,f}}_{\mathbf{k+1}} \end{bmatrix} = \begin{bmatrix} \mathbf{f}(\mathbf{x}^{\mathbf{i,a}}_{\mathbf{k}}, \mathbf{u_k}, \widehat{\theta}^{\mathbf{i,a}}_{\mathbf{k}}) \\ \mathbf{a}^{\mathbf{i,a}}_{\mathbf{k}} \\ \mathbf{h}(\mathbf{x}^{\mathbf{i,a}}_{\mathbf{k}}, \mathbf{u_k}) \end{bmatrix}, \tag{18}$$

2. *Assimilation*: The covariance matrix associated with the ensemble of augmented states is computed as:

$$\mathbf{C}^{\mathbf{f}}_{\mathbf{k+1}} = \frac{\left(\Xi^{\mathbf{f}}_{\mathbf{k+1}} - \overline{\mathbf{z}}^{\mathbf{f}}_{\mathbf{k+1}} \cdot \mathbf{1}^{\top}\right)\left(\Xi^{\mathbf{f}}_{\mathbf{k+1}} - \overline{\mathbf{z}}^{\mathbf{f}}_{\mathbf{k+1}} \cdot \mathbf{1}^{\top}\right)^{\top}}{R-1}, \tag{19}$$

where $\overline{\mathbf{z}}^{\mathbf{f}}_{\mathbf{k+1}} = \frac{1}{R}\sum_{i=1}^{R} \mathbf{z}^{\mathbf{i,f}}_{\mathbf{k+1}}$ is the average of the augmented states of the ensemble and $\mathbf{1}$ is the column vector with all the elements equal to 1. The Kalman gain then is defined as $\mathbf{K_{k+1}} = \mathbf{C}^{\mathbf{f}}_{\mathbf{k+1}}\mathbf{H}^{\top}(\mathbf{H}\mathbf{C}^{\mathbf{f}}_{\mathbf{k+1}}\mathbf{H}^{\top} + \mathbf{R_k})^{-1}$, with $\mathbf{R_k}$ the covariance matrix of the measurement noise. The states $\mathbf{z_k}$ are assimilated with the data $\mathbf{d_k}$ using the Kalman equations as follows:

$$\mathbf{z}^{\mathbf{i,a}}_{\mathbf{k+1}} = \mathbf{z}^{\mathbf{i,f}}_{\mathbf{k+1}} + \mathbf{K_{k+1}}(\mathbf{d_k} - \mathbf{H}\mathbf{z}^{\mathbf{i,f}}_{\mathbf{k+1}}). \tag{20}$$

In practice, the EnKF is implemented in a computationally more efficient fashion. Moreover it is often necessary to implement localization techniques to avoid spurious correlations. For details we refer to Evensen (2009) and Aanonsen et al. (2009).

Application case

In this section we perform a parameter estimation experiment where we compare the performance of the tensor parameterizations described in this paper with classical PCA parameterizations. We consider the data set provided by Vo and Durlofsky (2015), and construct an ensemble of $R = 100$ realizations of channelized reservoirs of size $I = 60$ and $J = 60$. The well configuration consists of 12 producer wells and 4 injectors, and their locations are depicted in **Fig. 5**. The producers are operated at a fixed bottom hole pressure and the injectors at fixed rates.
The field is producing for 15 years, with a simulation time step of $\Delta t = 1$ month. The measurements to be considered are the total rates at the producers, the bottom-hole pressures at the injectors and the fractional flows at the producers, with an observation time interval of 3 months. In the experiment, measurement errors are modeled as white noise, i.e. stochastic variables with a Gaussian distribution of zero mean. During the production stage, the petrophysical parameters are estimated with an interval of 2 years and the last update is made 6 years after the start of production. The key parameters for the experiment are summarized in **Table 1**. The forward simulations are performed with the Matlab Reservoir Simulation Toolbox (MRST), see, e.g., Lie et al. (2012). For the parameter estimation, we have used the EnKF module of MRST. We choose realization number 100 to be the truth. The permeability fields are represented in a tensor formulation $\mathcal{S}$ of size $60 \times 60 \times 99$ and we construct a set of low-dimensional representations $\Omega = \{\mathbf{a^1}, \mathbf{a^2}, \cdots, \mathbf{a^{99}}\}$, where $\mathbf{a} \in \mathbb{R}^{50}$, which is used as prior ensemble for the EnKF routine.

The plots of the total flow rates in several production wells, after the EnKF final update, are presented in **Figs. 6-8**. All of the plots consist of three figures, each one associated with the flow rates in a particular well for the parameter estimation result when using the unparameterized EnKF, the EnKF with tensor parameterization and the EnKF with PCA parameterization. The history matching period, which is depicted with a green background, ends after 6 years, and thereafter the reservoir models are used for prediction, during the time period depicted with a pink background. One of the principal objectives of the parameter estimation of reservoir models, of more importance than having a good history-match of the reservoir outputs, is to create an updated ensemble of

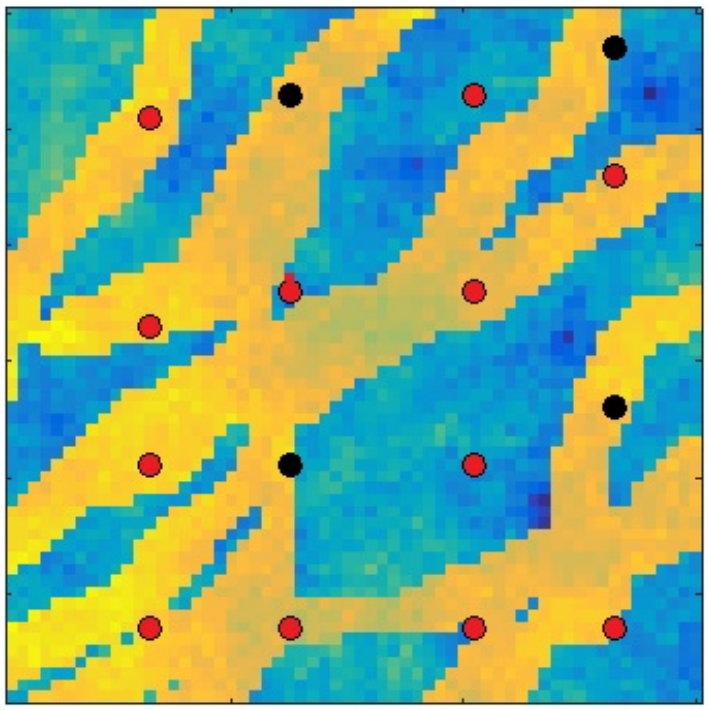

Figure 5: A realization of the permeability field and well configuration of the reservoir models. Red: Producer wells. Black: Injector wells.

reservoir models with good predictive capabilities. On the one hand, the EnKF without parameterization shows a very good history matching result. However, the updated ensemble of realizations presents very poor prediction capabilities for most of the wells. On the other hand, when the EnKF is used with low-dimensional tensor and the PCA parameterizations, it still generates good history matching results but now also results in considerably improved prediction capabilities. The poor prediction capability of the EnKF without parameterization can be explained from the loss of geological realism of the updated ensemble. In **Fig. 9** and **Fig. 10** we depict the final permeability updates of two realizations, using the methods described in this section. When no parameterization is used, the updates totally lose the channel structure. This is because the Kalman filter is only capable to capture the second-order statistics of the petrophysical properties. When tensor parameterizations are used, combined with an EnKF, they impose a certain amount of geological structure on the updates. Despite that the EnKF still only captures the second-order statistics, the geological updates have a structure imposed by the prior knowledge, which is included in the tensor basis functions, and as a result the geological updates still look like channelized reservoir models. The PCA updates lose much more of the geological realism of channelized structures compared to the results from the tensor updates.

Similar observations have been found for the watercuts. To exemplify, **Fig. 11** and **Fig. 12** show that the watercuts predicted by the EnKF with no parameterization are deviating from the truth, while the watercuts from the updated ensemble using a low-dimensional representation are able to predict more accurately the water breakthrough times.

Conclusion

In this paper we have analyzed the effectiveness of the parameterizations of petrophysical parameters with a tensor-based decomposition of the prior ensemble, for parameter estimation using CAHM, building on the work of Afra and Gildin (2013); Afra et.al. (2014); Afra and Gildin (2016). The efficiency of tensor approximations when representing channelized structures is illustrated by the fact that they require only 0.6% of the original

Parameter	Value	Unit
Simulation parameters		
Simulation time	15	[year]
Time step	1	[month]
Measurement errors, standard deviations		
Flow rates	12	$[m^3/day]$
Bottom-hole pressures	6	[bar]
Fractional flow (watercuts)	0.1	-
Parameter estimation experiment		
Observation time interval	3	[month]
Update time interval	2	[year]
End of history matching	6	[year]

Table 1–Details of the experimental setting.

amount of information to reconstruct channels appropriately, while a PCA approximation requires almost 63% (1 order of magnitude higher). In order to verify the potential use of the tensor approach for parameter estimation, our experiments involve the estimation of the permeability field of a channelized reservoir using three alternative parameterizations: grid block, PCA and tensor-based. The uncertainty space is covered by an ensemble of channelized realizations which are updated every two years. After the final history match, the updated ensemble is used to predict total rates, well pressures and water breakthrough times. For the case of grid block property updates (i.e., without parameterization), an excellent history match is observed, but the ensemble has poor prediction capabilities due to a loss of geological realism. When using tensor representations, we observe considerably improved prediction capabilities of the updated ensemble, outperforming the PCA approach, and an improved preservation of the geological realism of the updated ensemble.

Acknowledgements

The authors acknowledge financial support from the Recovery Factory program sponsored by Shell Global Solutions International.

References

Aanonsen, S.I., Nævdal, N., Oliver, D., Reynolds, A., Vallès, B., et al. 2009. The Ensemble Kalman Filter in Reservoir Engineering–a Review. *SPEJ* **14**(03): 393–412. DOI: 10.2118/117274-PA.

Afra, S. and Gildin, E. 2013. Permeability parametrization using Higher Order Singular Value decomposition (HOSVD). *12th International Conference on Machine Learning and Applications (ICMLA)* **2**: 188–193. DOI: 10.1109/icmla.2013.121.

Afra, S. and Gildin, E. 2014. Efficient inference of reservoir parameter distribution utilizing higher order SVD reparameterization. *ECMOR XIV-14th European Conference on the Mathematics of Oil Recovery.* DOI: 10.3997/2214-4609.20141826.

Afra, S., Gildin, E. and Tarrahi, M. 2014. Heterogeneous reservoir characterization ussing efficient parameterization through Higher Order SVD (HOSVD). *American Control Conference*: 147–152. DOI: 10.1109/acc.2014.6859246.

Afra, S. and Gildin, E. 2016. Tensor based geology preserving reservoir parameterization with Higher Order Singular Value Decomposition (HOSVD). *Computers & Geosciences* **94**: 110–120. DOI: 10.1016/j.cageo.2016.05.010.

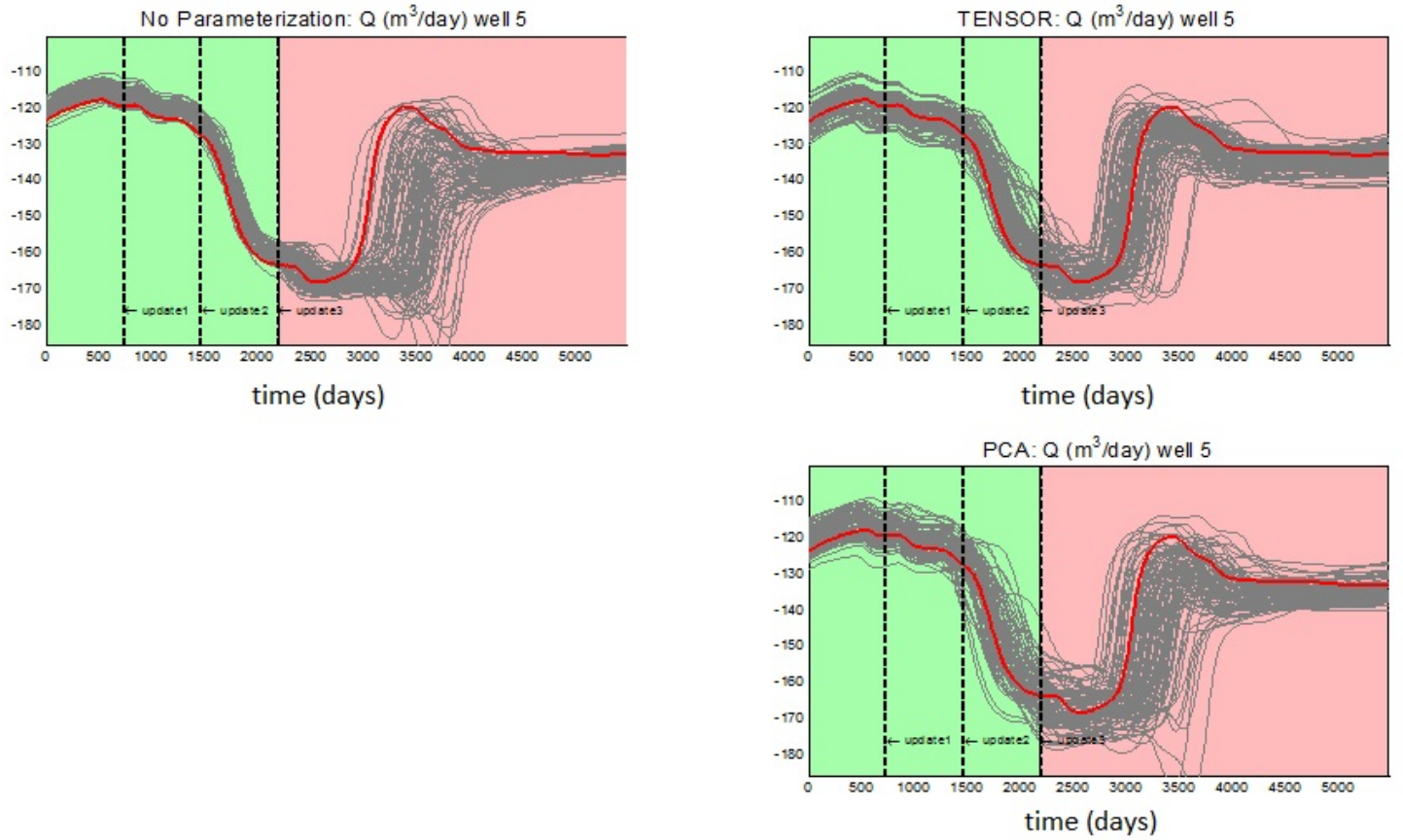

Figure 6: History matching and rate prediction. Total rates at well 5. The green background indicates the history matching interval. The pink background indicates the prediction interval. Red: Truth. Gray: Updated ensemble.

Bader, B.W., Kolda, T.G., et al. 2015. Matlab tensor toolbox version 2.6. URL: http://http://www.sandia.gov/ tgkolda/TensorToolbox/index-2.6.html.

Bro, R. 1997. PARAFAC. Tutorial and applications. *Chemometrics and Intelligent Laboratory Systems* **38**(2): 149–171. DOI: 10.1016/S0169-7439(97)00032-4.

Chen, C., Gao, G., Ramirez, B.A., Vink, J.C., Girardi, A.M. 2016. Assisted history matching of channelized models by use of Pluri-Principal-Component Analysis. *SPEJ* **21**(05): 793–812. DOI: 10.2118/173192-PA.

Chen, J. and Saad, Y. 2009. On the tensor SVD and the optimal low rank orthogonal approximation of tensors. *SIAM Journal on Matrix Analysis and Applications* **30**(4): 1709–1734. DOI:10.1137/070711621.

De Lathauwer, L., De Moor, B. and Vandewalle, J. 2000a. A multilinear singular value decomposition. *SIAM journal on Matrix Analysis and Applications* **21**(4): 1253–1278. DOI: 10.1137/s0895479896305696.

De Lathauwer, L., De Moor, B. and Vandewalle, J. 2000b. On the best rank-1 and rank-$(r_1, r_2, \cdots, r_n)$ approximation of higher-order tensors. *SIAM journal on Matrix Analysis and Applications* **21**(4): 1324–1342. DOI: 10.1137/s0895479898346995.

De Silva, V. and Lim, L.-H. 2008. Tensor rank and the ill-posedness of the best low-rank approximation problem. *SIAM Journal on Matrix Analysis and Applications* **30**(3): 1084–1127. DOI: 10.1137/06066518X.

Eckart, C. and Young, G. 1936. The approximation of one matrix by another of lower rank. *Psychometrika* **1**(3): 211–218. DOI: 10.1007/bf02288367.

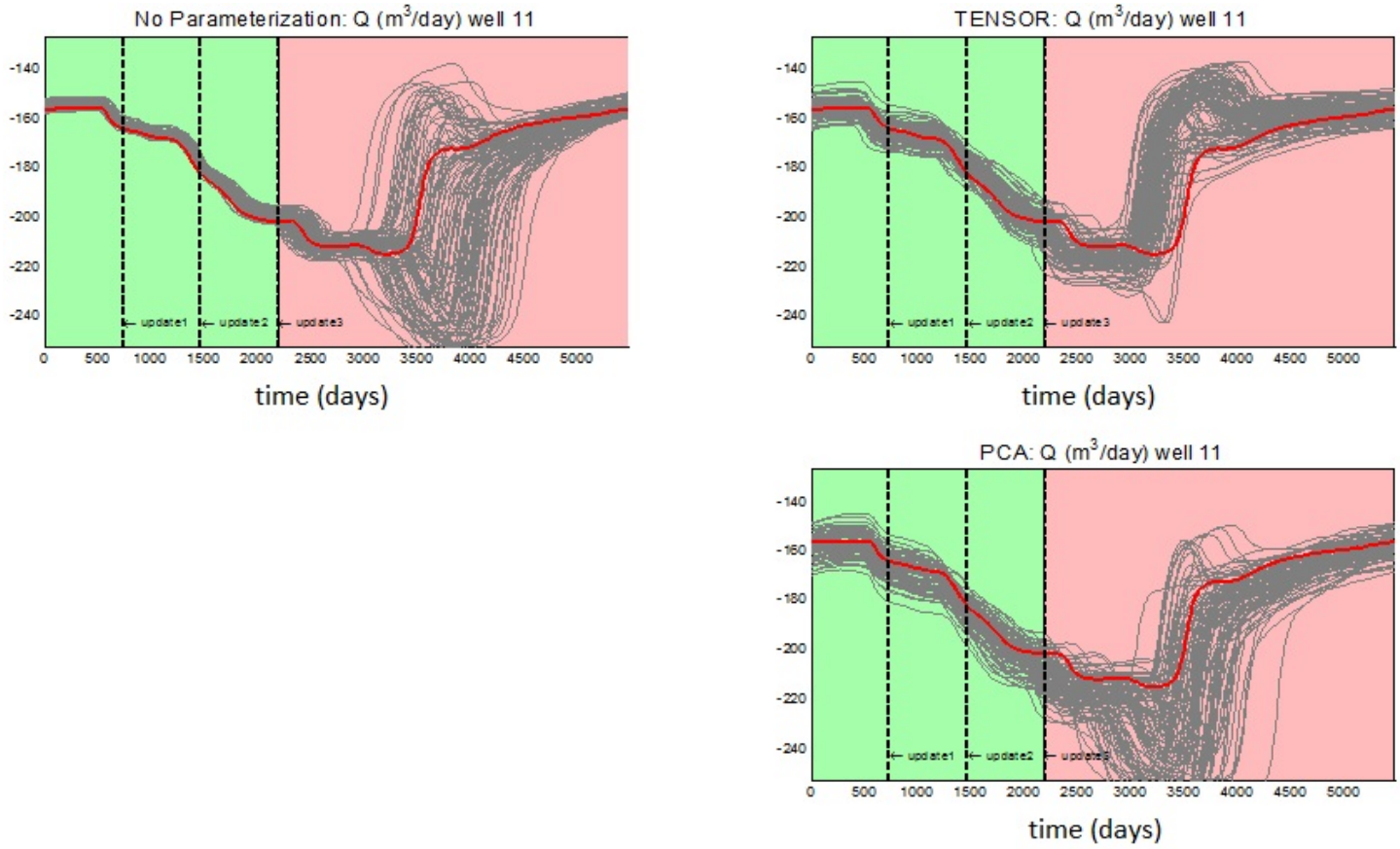

Figure 7: History matching and rate prediction. Total rates at well 11**. The green background indicates the history matching interval. The pink background indicates the prediction interval. Red: Truth. Gray: Updated ensemble.**

Evensen, G. 2009. *Data assimilation: The Ensemble Kalman filter*. Springer Science & Business Media. DOI: 10.1007/978-3-642-03711-5.

Golub, G.H. and Van Loan, C.F. 2012. *Matrix computations*, Volume 3. JHU Press. DOI: 10.1137/1032141

Harshman, R.A. 1970. Foundations of the PARAFAC procedure: Models and conditions for an "explanatory" multi-modal factor analysis. DOI: 10.1114/45652.

Harshman, R.A. and Lundy, M.E. 1994. PARAFAC: Parallel factor analysis. *Computational Statistics & Data Analysis* **18**(1): 39–72. DOI: 10.1016/0167-9473(94)90132-5.

Jafarpour, B., Goyal, V.K., McLaughlin, D.B., and Freeman, W.T. 2010. Compressed history matching: exploiting transform-domain sparsity for regularization of nonlinear dynamic data integration problems. *Mathematical Geosciences* **42**(1): 1–27. DOI: 10.1007/s11004-009-9247-z.

Jafarpour, B., McLaughlin, D.B., et al. 2009. Reservoir characterization with the Discrete Cosine Transform. *SPEJ* **14**(01): 182–201. DOI: 10.2118/106453-PA.

Jansen, J.D., Fonseca, R.M., Kahrobaei,S., Siraj, M.M., Van Essen, G.M., and Van den Hof, P.M.J. 2014. The egg model–a geological ensemble for reservoir simulation. *Geoscience Data Journal* **1**(2): 192–195. DOI: 10.1002/gdj3.21.

Kolda, T.G. and Bader, B.W. 2009. Tensor decompositions and applications. *SIAM review* **51**(3): 455–500. DOI: 10.1137/07070111X.

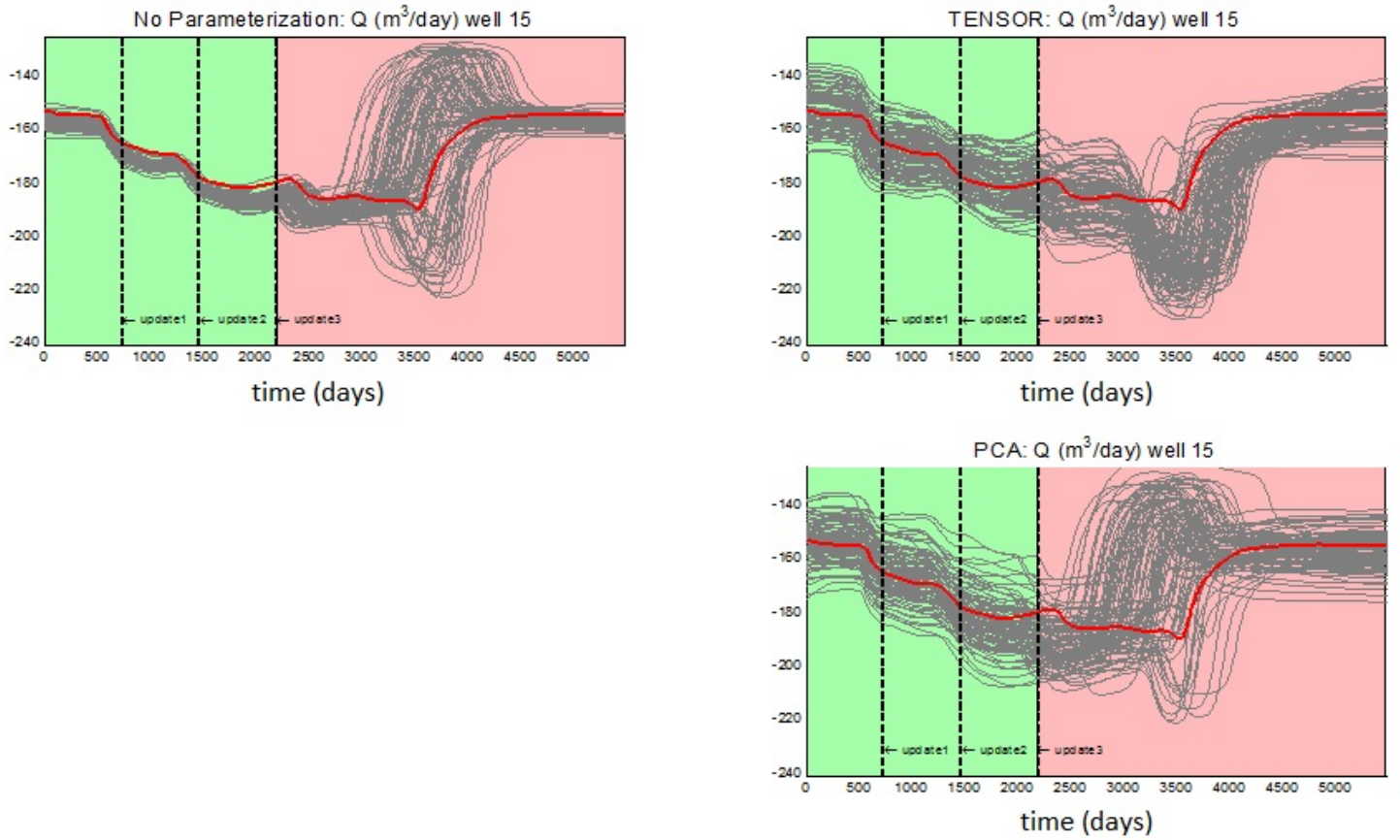

Figure 8: History matching and rate prediction. Total rates at well 15**. The green background indicates the history matching interval. The pink background indicates the prediction interval. Red: Truth. Gray: Updated ensemble.**

Lie, K.A., Krogstad, S., Ligaarden, I.S., Natvig, J.R., Nilsen, H.M, and Skaflestad, B. 2012. Open-source matlab implementation of consistent discretisations on complex grids. *Computational Geosciences* **16**(2): 297–322. DOI: 10.1007/s10596-011-9244-4.

Lim, L.-H. 2004. Whats possible and whats not possible in tensor decompositions–A freshmans view. In *Workshop on Tensor Decompositions, American Institute of Mathematics*. URL: https://www.stat.uchicago.edu/ lekheng/work/td.pdf

Oliver, D. 1996. Multiple realizations of the permeability field from well test data. *SPEJ* **1**(02): 145–154. DOI: 10.2118/27970-PA.

Oliver, D., Reynolds, A., and Liu, N., 2008. *Inverse theory for petroleum reservoir characterization and history matching*. Cambridge University Press. DOI: 10.1017/CBO9780511535642.

Oliver, D.S. and Chen,Y. 2011. Recent progress on reservoir history matching: A review. *Computational Geosciences* **15**(1): 185–221. DOI: 10.1007/s10596-010-9194-2.

Reynolds, A., He, N., Chu, L., Oliver, D., et al. 1996. Reparameterization techniques for generating reservoir descriptions conditioned to variograms and well-test pressure data. *SPEJ* **1**(04): 413–426. DOI: 10.2118/30588-PA.

Sahni, I., Horne, R.N., et al. 2005. Multiresolution wavelet analysis for improved reservoir description. *SPE Reservoir Evaluation & Engineering* **8**(01): 53–69. DOI: 10.2118/87820-PA.

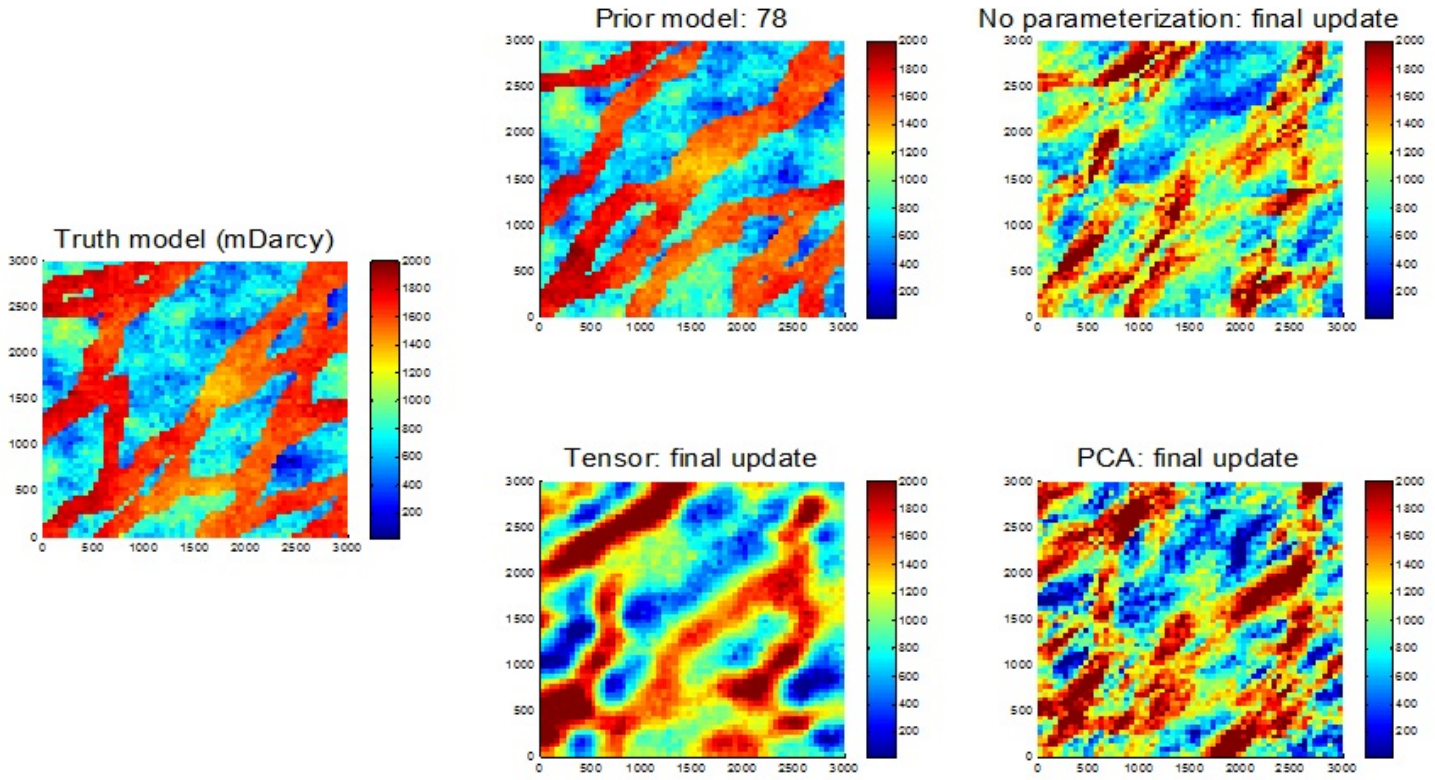

Figure 9: Final update permeability field, realization 78**.**

Sarma, P., Chen, W.H., Durlofsky, L.J., Aziz, K. et al. 2008. Production optimization with adjoint models under nonlinear control-state path inequality constraints. *SPE Reservoir Evaluation & Engineering 11*(02): 326–339. DOI: 10.2118/99959-PA.

Shekhawat, H. and Weiland S. 2014. On the problem of low rank approximation of tensors. In 21st *International Symposium on Mathematical Theory of Networks and Systems.*, Groningen, The Netherlands. URL: http://fwn06.housing.rug.nl/mtns2014-papers/fullPapers/0386.pdf.

Tavakoli, R., Reynolds, A., et al. 2010. History matching with parametrization based on the SVD of a dimensionless sensitivity matrix. *SPEJ* **15**(02): 495–508. DOI: 10.2118/118952-PA.

Tucker, L.R. 1966. Some mathematical notes on three-mode factor analysis. *Psychometrika* **31**(3): 279–311. DOI: 10.1007/BF02289464.

Van Belzen, F. 2011. *Approximation of multi-variable signals and systems: a tensor decomposition approach*. Ph. D. thesis, PhD thesis, Eindhoven University of Technology, The Netherlands. DOI: 10.6100/IR712120.

Van Belzen, F. and Weiland, S. 2012. A tensor decomposition approach to data compression and approximation of *N*d systems. *Multidimensional Systems and Signal Processing* **23**: 209–236. DOI: 10.1007/s11045-010-0144-x.

Van Doren, J.F., Douma, S.G., Van den Hof, P.M.J., Jansen, J.D. and Bosgra, O.H. 2009. Identifiability: from qualitative analysis to model structure approximation. *IFAC Proceedings Volumes* **42**(10): 664–669. DOI: 10.3182/20090706-3-FR-2004.00110.

Van Doren, J.F., Van den Hof, P.M.J., Jansen, J.D. and Bosgra, O.H. 2011. Parameter identification in large-scale models for oil and gas production. *IFAC Proceedings Volumes* **44**(1): 10857–10862. DOI: 10.3182/20110828–6–it–1002.01823.

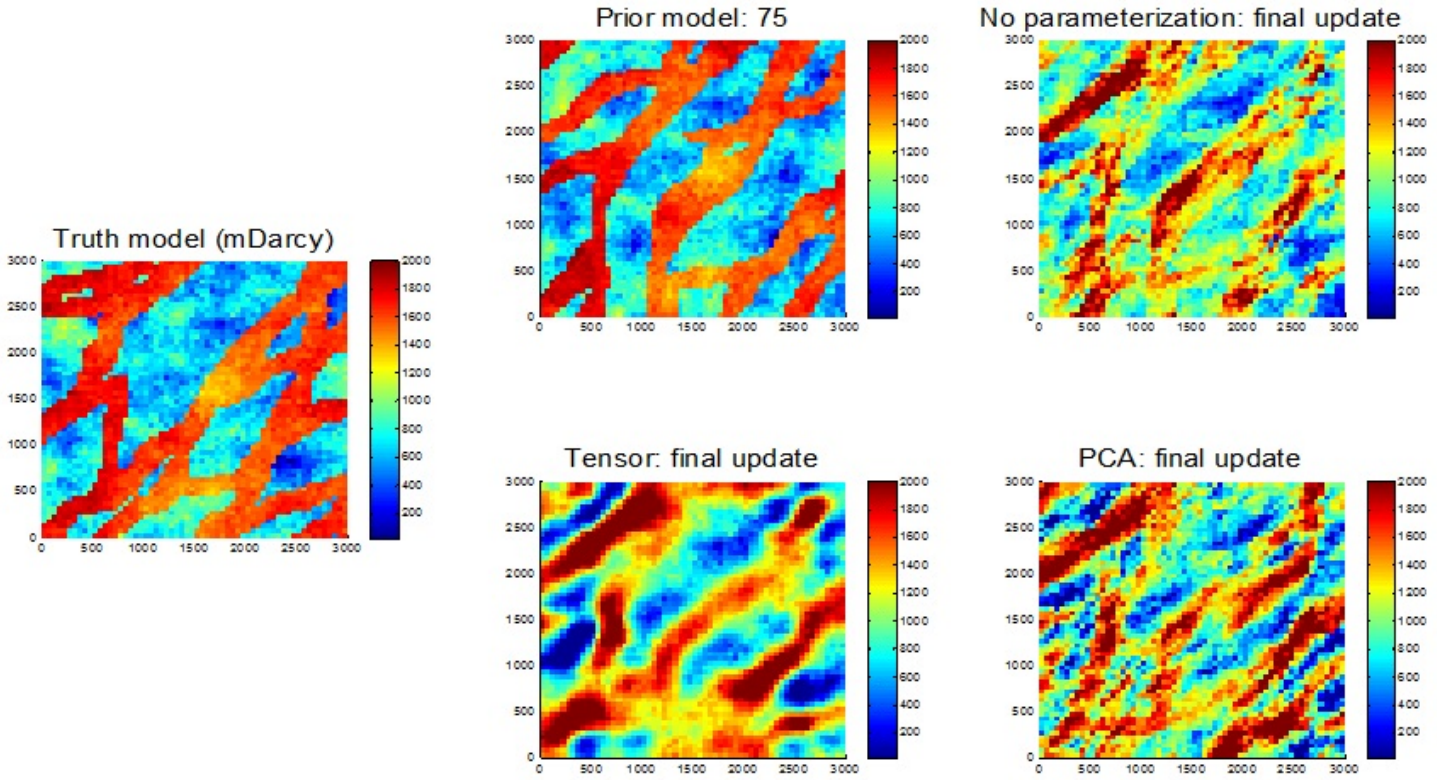

Figure 10: Final update permeability field, realization 75**.**

Van Essen, G.M., Kahrobaei, S., van Oeveren, H., Van den Hof, P.M.J. and Jansen, J.D. 2016. Determination of lower and upper bounds of predicted production from history-matched models. *Computational Geosciences* **20**(1061). DOI: 10.1007/s10596-016-9576-1.

Vervliet, N., Debals, O., Sorber, L., Van Barel, M., and De Lathauwer, L. 2016. Tensorlab v3.0. URL: http://www.tensorlab.net/.

Vo, H.X. and Durlofsky, L.J. 2015. Data assimilation and uncertainty assessment for complex geological models using a new PCA-based parameterization. *Computational Geosciences* **19**(4): 747–767. DOI: 10.1007/s10596-015-9483-x.

Weiland, S. and Van Belzen, F. 2010. Singular value decompositions and low rank approximation of tensors. *IEEE Transactions on Signal Processing* **58**(3): 1171–1182. DOI: 10.1109/tsp.2009.2034308.

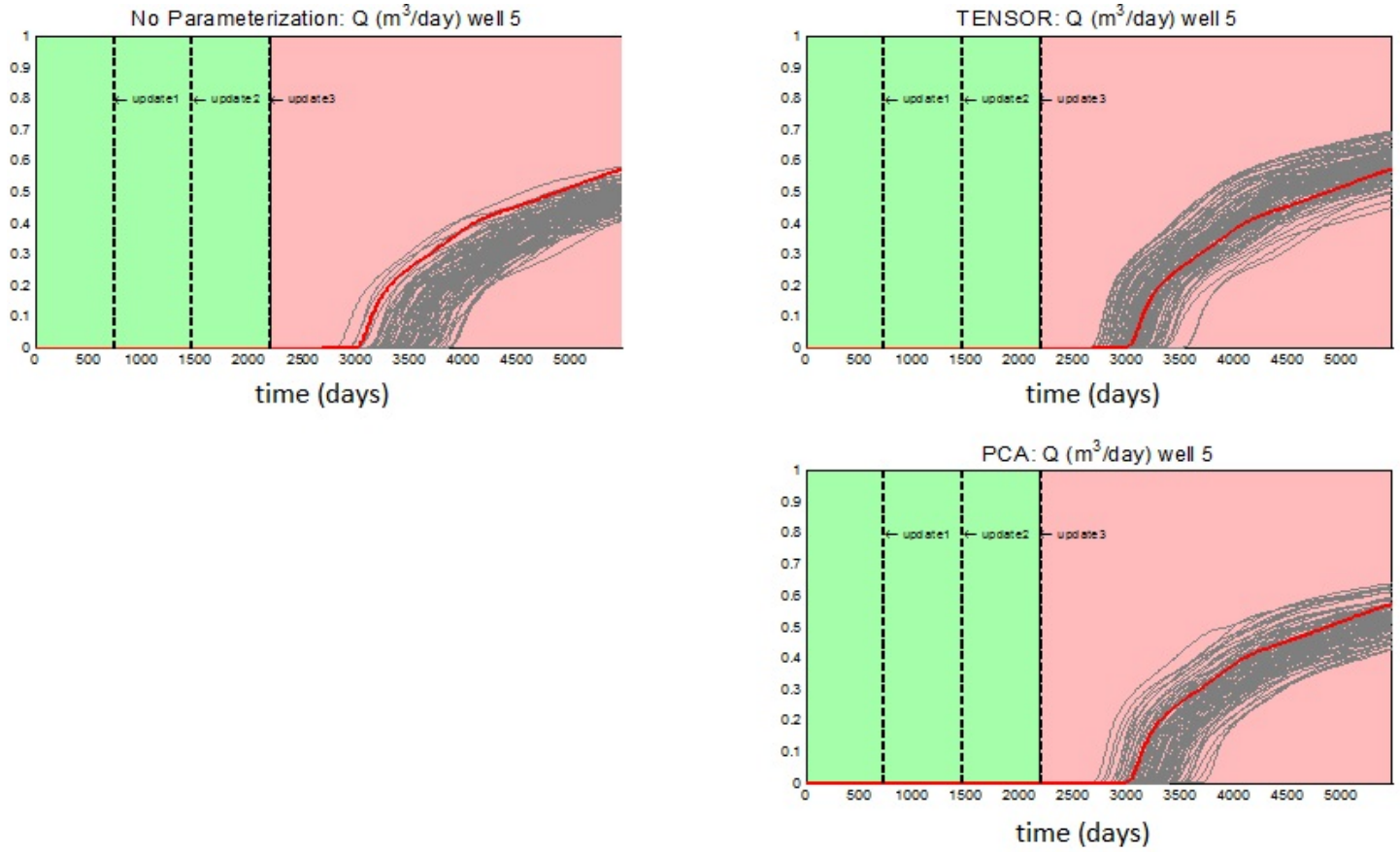

Figure 11: History matching and water breakthrough prediction. Fractional flow at well 5. The green background indicates the history matching interval. The pink background indicates the prediction interval. Red: Truth. Gray: Updated ensemble.

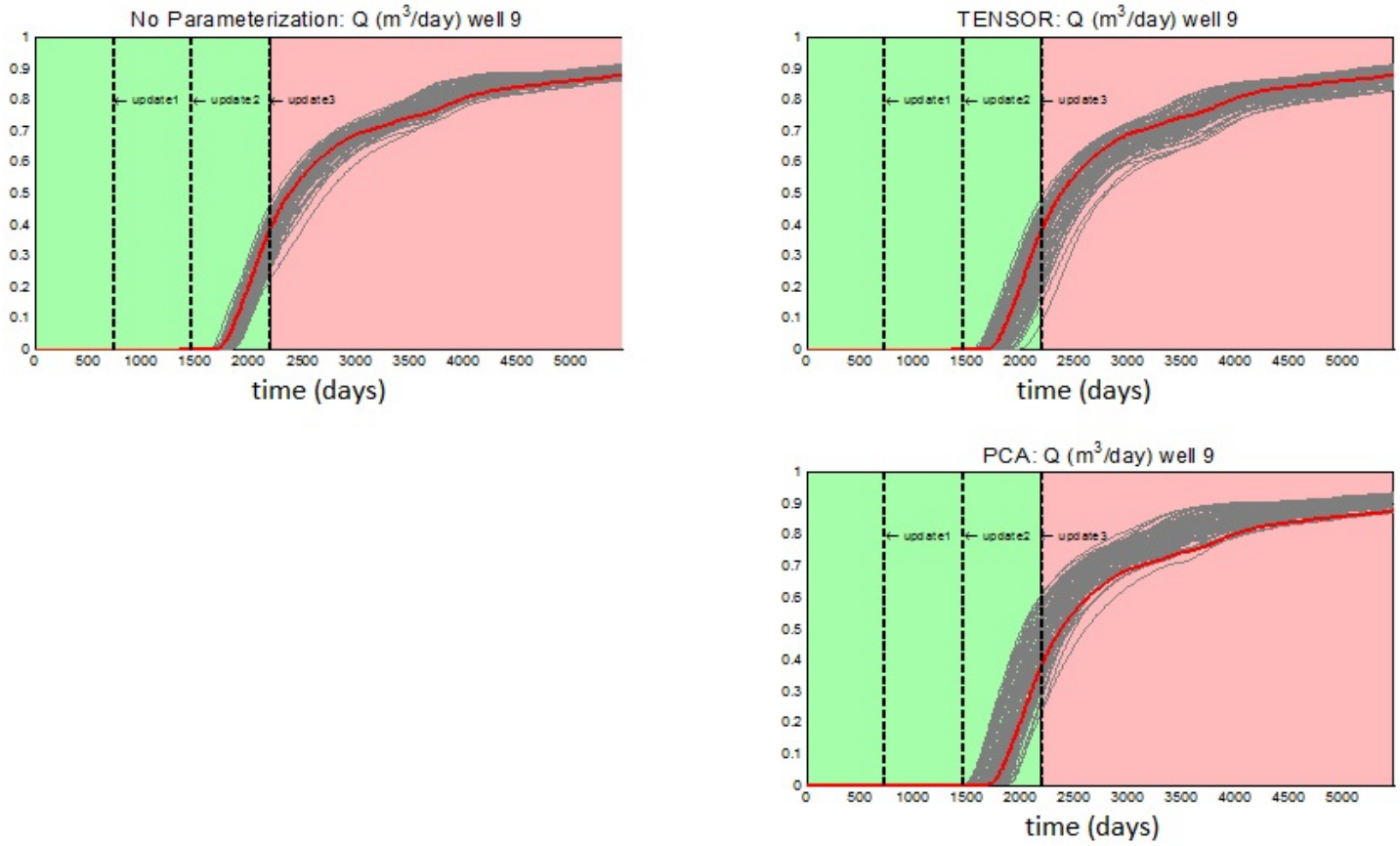

Figure 12: History matching and water breakthrough prediction. Fractional flow at well 9. The green background indicates the history matching interval. The pink background indicates the prediction interval. Red: Truth. Gray: Updated ensemble.